



AIAS 2017 International Conference on Stress Analysis, AIAS 2017, 6-9 September 2017, Pisa, Italy

Sensibility analysis of the fatigue critical distance values assessed by combining plain and notched cylindrical specimens

C. Santus^{a,*}, D. Taylor^b, M. Benedetti^c

^aDepartment of Civil and Industrial Engineering, University of Pisa, Pisa, Italy

^bDepartment of Mechanical & Manufacturing Engineering, Trinity College Dublin, Dublin, Ireland

^cDepartment of Industrial Engineering, University of Trento, Trento, Italy

Abstract

The material critical distance is often deduced from plain and notched specimens, instead of experimentally measuring the (long) crack threshold, which is a challenging task and not adequate in some cases. A dedicated V-notched specimen was proposed along with a dimensionless numerical procedure to derive the critical distance from the fatigue stress concentration factor, by implementing both the line and the point methods. An experimental validation activity is provided here on 42CrMo4+QT steel, focusing on how the critical distance result is sensitive to the actual local radius, the specimen sharpness, and the choice between the line or the point method. The determination of the critical distance with the point method systematically provides higher values than the line method. However, these length discrepancies do not produce large effects in terms of the component strength assessment if the same method for the fatigue limit evaluation is used. By alternatively considering the specimen not involved in the critical distance determination, as a potential design component, the prediction accuracy was evaluated. This analysis confirmed that a small notch radius is recommended for the fatigue strength assessment of larger radius notches or even of a crack, whereas by deducing the critical distance from a blunt notch, a noticeable inaccuracy can be found on smaller radius and crack threshold.

Copyright © 2018 The Authors. Published by Elsevier B.V.

Peer-review under responsibility of the Scientific Committee of AIAS 2017 International Conference on Stress Analysis

Keywords: Critical distance determination; Line and point methods; 42CrMo4+QT steel; Rounded V-notched specimen; Sharp and blunt notches

* Corresponding author. Tel.: +39-050-2218007; fax: +39-050-2210604.

E-mail address: ciro.santus@ing.unipi.it

Nomenclature

| | |
|-----------------------|---|
| ΔK_{th} | Threshold stress intensity factor, full range. |
| $\Delta\sigma_{fl}$ | Plain specimen fatigue limit, full range. |
| L | Fatigue critical distance. |
| $\Delta\sigma_{N,fl}$ | Notched specimen fatigue limit, nominal stress, full range. |
| K_f | Fatigue stress concentration factor. |
| D | Specimen external diameter. |
| R | Notch radius. |
| A | Notch depth. |
| ρ | R/A notch radius ratio. |
| α | Notch angle. |
| l_{min}, l_{max} | Minimum and maximum critical distance accuracy range limits. |
| R | Fatigue load ratio |
| $L_{-1}, L_{0.1}$ | Experimental critical distances for the load ratios -1 and 0.1. |

1. Introduction

The strength of notched components, both under fatigue loading and monotonic brittle fracture, can be evaluated with the Theory of Critical Distances (Taylor (2007), Taylor (2008)) and different methods can be formalized within the framework of this theory. Among them, the Line Method and the Point Method are the simplest and most commonly used, assuming the maximum principal stress as criterion. When multiaxial fatigue is involved, the Point method may be preferential, such as for the fretting application (Araújo et al. (2007), Bertini and Santus (2015)), while the Line method can better consider the residual stress field (Benedetti et al. (2010), Benedetti et al. (2016)).

According to its basic definition, the Critical Distance length is obtained by combining the threshold stress intensity factor full range ΔK_{th} and the plain specimen fatigue limit full range $\Delta\sigma_{fl}$:

$$L = \frac{1}{\pi} \left(\frac{\Delta K_{th}}{\Delta\sigma_{fl}} \right)^2 \quad (1)$$

However, an accurate measurement of the threshold may be a challenging experiment, moreover, the status of the material at the crack tip is different from the machined condition typical of any component notch and, for some materials, this may cause inaccuracy in terms of strength assessment. For these reasons, any sharply notched specimen can be considered as an alternative of the fracture mechanics testing to evaluate the L value (Taylor (2011)), or ultimately to obtain the threshold after Eq. 1 inversion. This approach has been emphasized by Susmel and Taylor (2010) finding both the threshold and the fracture toughness for a large variety of materials and fatigue load ratios.

The use of a sharp V-notched specimen has been recently proposed by Santus et al. (2017), providing a formulation to straightforwardly calculate the critical distance. After briefly presenting this procedure, experimental fatigue limits and thresholds are provided for 42CrMo4+QT steel under load ratios -1 and 0.1, then assessment analyses are performed and results discussed.

2. Critical distance determination

Two similar procedures were proposed by implementing both the Line and the Point methods, as summarized in Fig. 1. The analysis is expressed in dimensionless form, and a first length is analytically obtained just by assuming the singularity term solution. This length is calculated introducing the unitary N-SIF ($K_{N,UU}$) and the fatigue stress

concentration factor (K_f), which is the only experimental input of the procedure. This initial length may not be an accurate assessment of the actual critical distance. A correction function is therefore introduced to consider the notch root radius, which in turn allowed the definition of an inverse function. This turned out to be conveniently modeled just as a linear relationship for the Line Method (LM), while a 4th degree polynomial was required for the Point Method (PM). The coefficients for implementing this procedure were obtained from a series of accurate simulations, not reported here for brevity, avoiding the need of a finite element simulation of the specific specimen.

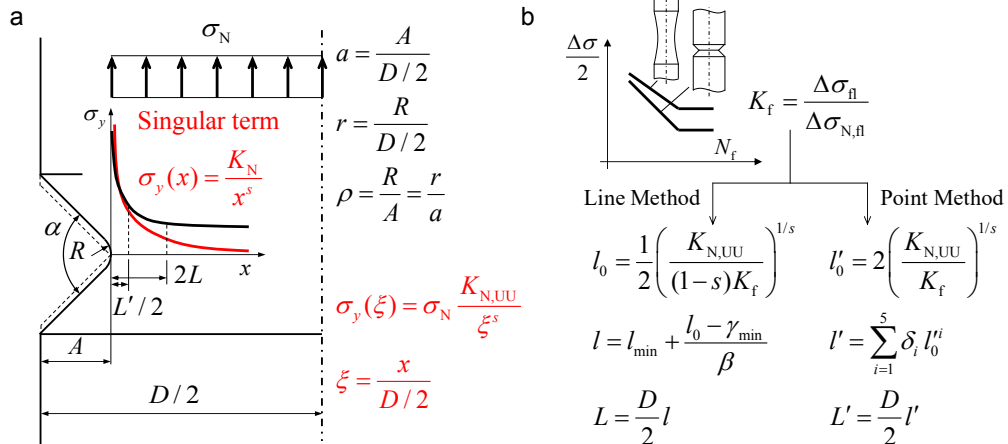


Fig. 1. (a) V-notch root stress distribution and specimen dimensions; (b) Line and Point method inverse search procedures.

The LM correction function was also considered for defining the limits of a range in which the inversion is accurate, or at least less sensitive to any material or experimental issues. By imposing minimum and maximum values of the inverse function, l_{\min} and l_{\max} were obtained. If the critical distance to be found is either too small or too large, and therefore near these limits or even outside the range, small variations of the fatigue limit causes large variation of the deduced critical distance, Fig. 2. When L is small, such as for a high strength steel as investigated in this paper, the notch radius may be the limiting factor being required to be manufactured quite small as well. On the contrary, for large critical distance materials, such as a gray cast iron, the specimen size needs to be relatively large while the local radius is less critical, however this latter situation is not such typical for structural metals.

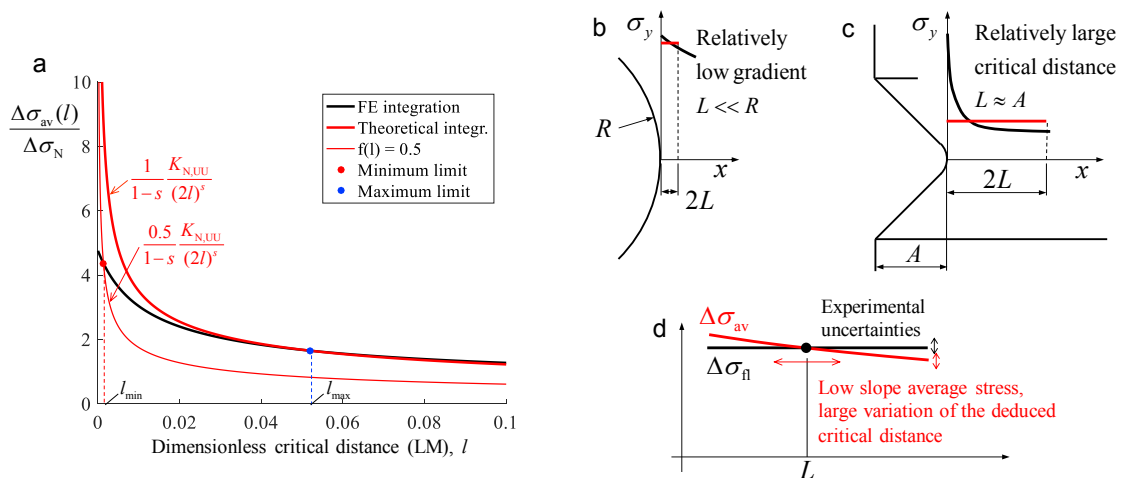


Fig. 2. (a) Correction function and accurate inverse search range; (b-c-d) Inaccurate determination outside, or near, the range limits.

3. Sensitivity

The sensitivity of the inverse search problem, where the unknown is the length L , can be defined as the effect on the critical distance for any variation of the experimental input which is the fatigue stress concentration factor K_f . A derivative definition can be proposed, Eq. 2, and, as evident in Fig. 3 (a), this sensitivity has a minimum in the $l_{min} - l_{max}$ range and it is lower for a sharper notch especially at lower values of the critical distance itself.

$$S = -\frac{1}{L} \frac{dL}{dK_f} = -\frac{1}{l} \frac{dl}{dK_f} \tag{2}$$

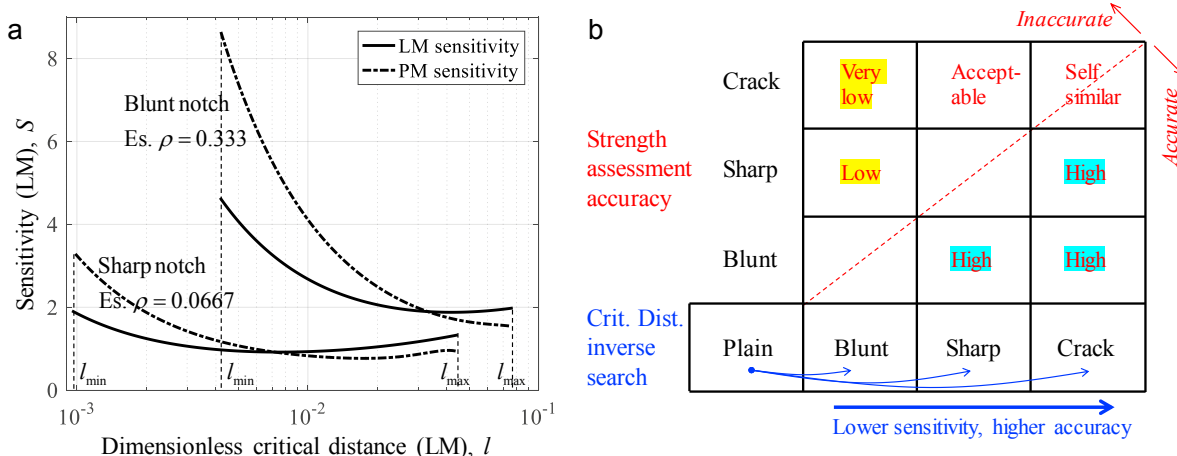


Fig. 3. (a) Sensitivity functions for blunt and sharp notches; (b) Accuracy map of the critical distance and the fatigue strength assessments.

Fig. 3 (b) shows an accuracy assessment map for a small critical distance situation that can be deduced from the sensitivity just introduced: by combing the plain fatigue limit with the strength of a sharp specimen (or even the crack threshold) a good estimate of the critical distance is obtained, being less sensitive to any potential bias; on the contrary, if the critical distance is evaluated with a blunt notched specimen, a large discrepancy of the critical distance can result. Assuming the other specimen as a design component for which the strength should be assessed, the accuracy of the critical distance evaluation can be effectively quantified in terms of the fatigue limit prevision. The evaluation of the blunt notch is expected to be accurate with either sharp or crack threshold derived critical distances, while a large stress difference between the experimental fatigue limit and the assessed value can result about the sharp notch if the length L is evaluated with the blunt specimen. Obviously, the crack threshold, the sharp and the blunt fatigue limits could even be in perfect agreement, leaving these trends not evident. However, this situation is only hypothetical, indeed these variations have been found, quite clearly, by elaborating and comparing the experimental data reported below.

4. Experiment

Though a quite common steel was investigated, the literature data was not considered to avoid any material source of inconsistency. All the specimens for the tests were extracted from laminated bars (63 mm diameter) in 42CrMo4+QT which was provided as a unique supply to avoid any material mismatch due to slightly different heat treatment or material composition, and they were: tensile test specimen, plain specimen, sharp and blunt V-notched specimens, C(T) and M(T) specimens according to the standard ASTM E647 – 15, Fig. 4 (a). The C(T) specimen was used to measure the crack growth rate under the load ratio 0.1, while the data for the load ratio -1 was obtained with the M(T) specimen. The drawing of the sharp notched specimen is shown Fig. 4 (b) with a local radius quite

small $R = 0.2$ mm, and a SEM visualization after section cut was performed to verify the accuracy of this dimension, Fig. 4 (c). Since the expected critical distance for this kind of material is in the order of a few tens of microns, even a smaller radius would be recommended, however a tool nose radius lower than 0.2 mm was difficult to find. The same drawing was also considered for the blunt specimen, however with 1.0 mm root radius, which was (intentionally) much larger than the expected critical distance, reproducing the situation of Fig. 2 (b).

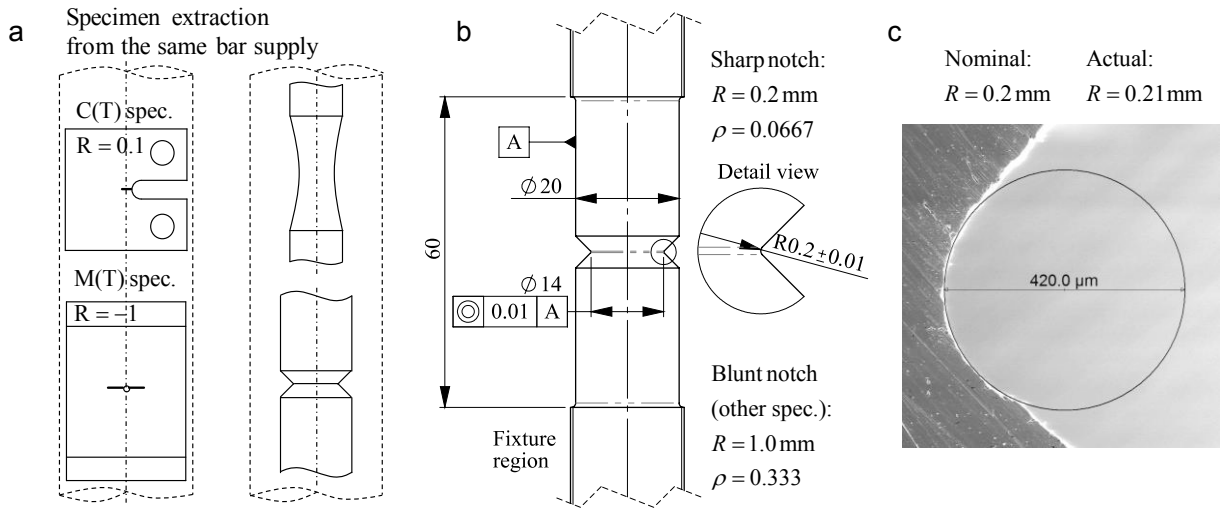


Fig. 4. (a) Specimen extraction from bars; (b) V-notched specimen drawing; (c) Visualization of the actual notch radius by SEM.

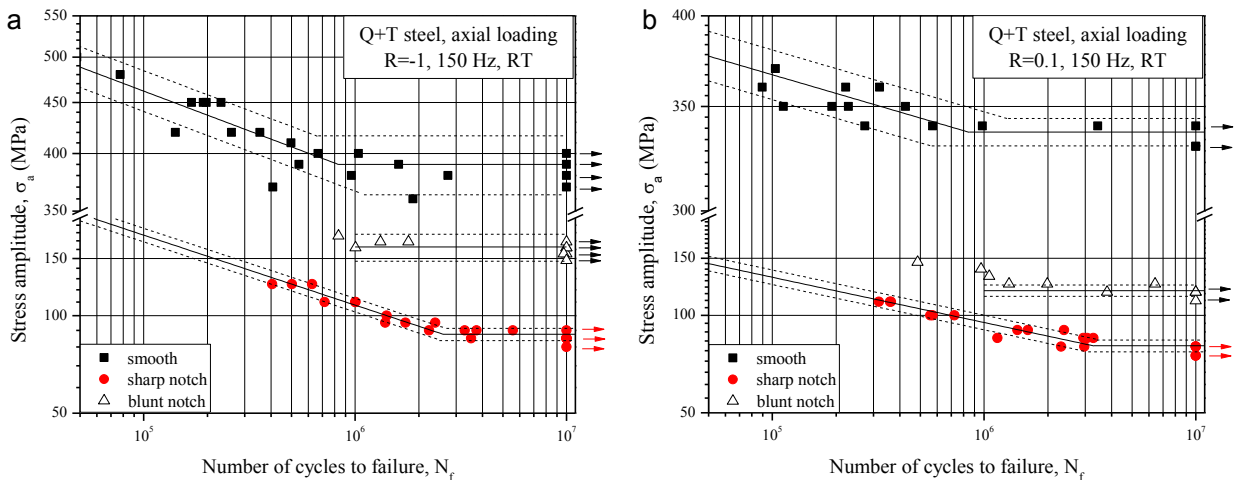


Fig. 5. (a) $R = -1$, (b) $R = 0.1$ fatigue data and fit lines of plain (smooth), and blunt and sharp notches.

Typical quenched and tempered steel tensile test properties were found: Yield and Ultimate 727 ± 13 MPa, 875 ± 15 MPa respectively, percentage elongation at fracture $17.6 \pm 0.25\%$, and reduction of area $57.7 \pm 0.43\%$, in agreement with the standard EN 10083-3:2006. The obtained fatigue test results are reported in Fig. 5 (a) and (b) for the load ratios -1 and 0.1 respectively and for the plain (smooth), the sharp ($R = 0.21$ mm) and the blunt ($R = 1.0$ mm) specimens. For brevity, the crack growth curves are not reported, however the threshold stress intensity factor ranges are listed in Table 1 along with all the cylindrical specimen fatigue limits and their standard deviations.

Table 1. Crack threshold and plain, blunt and sharp specimen fatigue limits for R = -1 and R = 0.1 load ratios.

| R = -1 | | | R = 0.1 | | |
|---|-------------------------------------|-------------------------------------|---|-------------------------------------|-------------------------------------|
| $\Delta K_{th} = 9.1 \text{ MPa m}^{0.5}$ | | | $\Delta K_{th} = 7.2 \text{ MPa m}^{0.5}$ | | |
| Plain $\Delta\sigma_{pl}/2$, MPa | Blunt $\Delta\sigma_{N,pl}/2$, MPa | Sharp $\Delta\sigma_{N,pl}/2$, MPa | Plain $\Delta\sigma_{pl}/2$, MPa | Blunt $\Delta\sigma_{N,pl}/2$, MPa | Sharp $\Delta\sigma_{N,pl}/2$, MPa |
| 390 (50%) | 163 (50%) | 87.5 (50%) | 337 (50%) | 119 (50%) | 80.5 (50%) |
| 20.7 (St. dev.) | 12.1 (St. dev.) | 2.9 (St. dev.) | 5.3 (St. dev.) | 3.7 (St. dev.) | 2.7 (St. dev.) |

5. Results analysis

5.1. Critical distance evaluation

The critical distance determination with the analytical procedure briefly described above was applied considering the notch fatigue factor both for the sharp and the blunt specimens at the two analyzed load ratios, and then the obtained lengths were compared to the values deduced from the thresholds. This comparative analysis is reported in Table 2 and graphically in Fig. 6. A variation of the actual radius, in the range of the drawing tolerance, from $R = 0.2$ (nominal) to $R = 0.21$ (actual), produces a quite small effect in terms of critical distance output, approximately on the order of 5%, Fig. 6 (a). More evident is the effect of the method considered. The length obtained with the point method is systematically larger than the value obtained with the line method and the relative ratio is almost a factor of two. The threshold deduced length was intermediate for the load ratio -1, just slightly closer to the point method value, while a more accurate prediction was obtained by the line method for the load ratio 0.1, Fig. 6 (b).

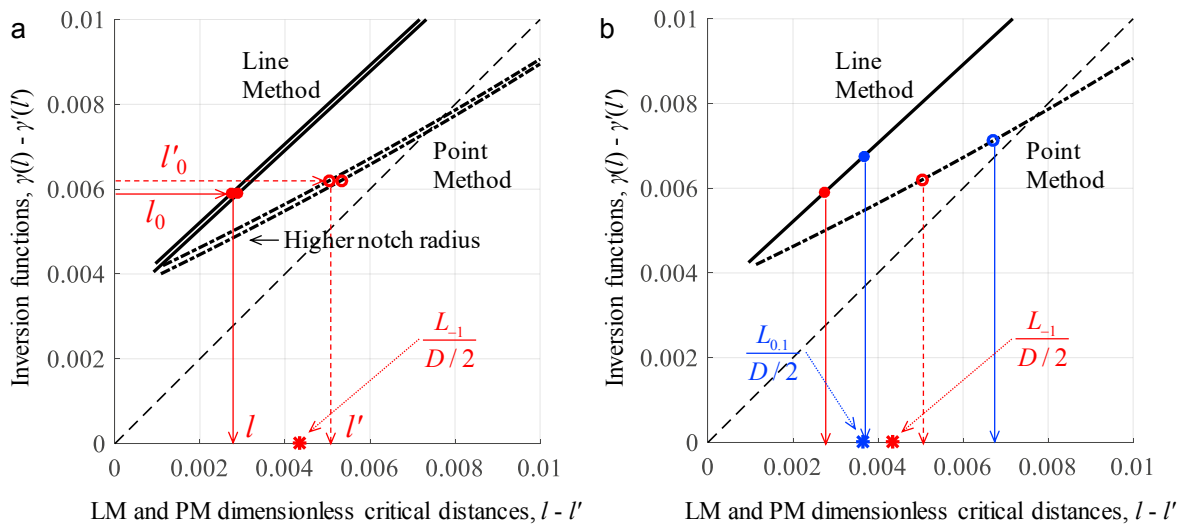


Fig. 6. Critical distance determination: (a) notch radius variation effect for the load ratio -1, (b) inverse search for the load ratios -1 and 0.1.

Table 2. Comparison between the threshold critical distances vs. the sharp and the blunt specimen derived values.

| R = -1 | | | | R = 0.1 | | | |
|--|-----------|---------------|-----------|---|-----------|---------------|-----------|
| Plain - ΔK_{th} , $L_{-1} = 0.0433 \text{ mm}$ | | | | Plain - ΔK_{th} , $L_{0.1} = 0.0363 \text{ mm}$ | | | |
| Plain - Sharp | | Plain - Blunt | | Plain - Sharp | | Plain - Blunt | |
| LM | PM | LM | PM | LM | PM | LM | PM |
| 0.0273 mm | 0.0505 mm | 0.0970 mm | 0.1836 mm | 0.0367 mm | 0.0671 mm | 0.0078 mm | 0.0063 mm |
| -36.9% | 16.6% | 123.8% | 323.9% | 1.1% | 84.7% | -78.5% | -82.5% |

The prediction with the blunt specimen is also reported in Table 2, and large differences were obtained: much larger critical distances for load ratio -1, and too small values for load ratio 0.1 even lower than the minimum range limit previously introduced.

5.2. Fatigue strength assessment

The critical distance material property is used to evaluate the fatigue strength at the design stage, therefore a better measure of the accuracy should be defined as the fatigue limit prediction of a structural component, or a different kind of specimen, rather than the value of the critical distance itself.

After having deduced the critical distance length either from the sharp or the blunt specimen, the estimated threshold stress intensity factor range was easily obtained by reversing Eq. 1. The results of this analysis are reported in Table 3 and the assessed thresholds are then compared with the experimental values. In agreement with the accuracy map reported in Fig. 3 (b), the crack fatigue strength was quite correctly predicted by the sharp specimen especially with the Point Method for $R = -1$ and the Line Method for $R = 0.1$. The discrepancies reported in Table 3 are obviously in agreement with the critical distance length assessments in Table 2, however with lower percentages, approximately reduced by a factor of two.

Table 3. Crack threshold ranges compared with the sharp and the blunt specimen derived values.

| R = -1 | | $\Delta K_{th} = 9.1 \text{ MPa m}^{0.5}$ | | R = 0.1 | | $\Delta K_{th} = 7.2 \text{ MPa m}^{0.5}$ | |
|---------------------------|---------------------------|---|---------------------------|---------------------------|---------------------------|---|---------------------------|
| Plain - Sharp | | Plain - Blunt | | Plain - Sharp | | Plain - Blunt | |
| LM | PM | LM | PM | LM | PM | LM | PM |
| 7.23 MPa m ^{0.5} | 9.82 MPa m ^{0.5} | 13.6 MPa m ^{0.5} | 18.7 MPa m ^{0.5} | 7.24 MPa m ^{0.5} | 9.78 MPa m ^{0.5} | 3.34 MPa m ^{0.5} | 3.01 MPa m ^{0.5} |
| -20.6% | 8.0% | 49.6% | 105.9% | 0.5% | 35.9% | -53.6% | -58.2% |

Table 4. Fatigue limit assessments of the sharp and the blunt specimens obtained with different critical distance evaluations.

| Results obtained with Plain - <i>Threshold</i> critical distances | | | | | | | |
|---|-----------|---|----------|---|-----------|--|-----------|
| R = -1, Sharp | | R = 0.1, Sharp | | R = -1, Blunt | | R = 0.1, Blunt | |
| $\Delta\sigma_{N_i}/2 = 87.5 \text{ MPa}$ | | $\Delta\sigma_{N_i}/2 = 80.5 \text{ MPa}$ | | $\Delta\sigma_{N_i}/2 = 163 \text{ MPa}$ | | $\Delta\sigma_{N_i}/2 = 119 \text{ MPa}$ | |
| LM | PM | LM | PM | LM | PM | LM | PM |
| 96.9 MPa | 85.0 MPa | 80.3 MPa | 71.3 MPa | 148.4 MPa | 143.1 MPa | 126.5 MPa | 122.8 MPa |
| 10.8% | -2.8% | -0.2% | -11.4% | -9.0% | -12.2% | 6.3% | 3.2% |
| Results obtained with Plain - <i>Blunt</i> critical distances | | | | Results obtained with Plain - <i>Sharp</i> critical distances | | | |
| R = -1, Sharp | | R = 0.1, Sharp | | R = -1, Blunt | | R = 0.1, Blunt | |
| $\Delta\sigma_{N_i}/2 = 87.5 \text{ MPa}$ | | $\Delta\sigma_{N_i}/2 = 80.5 \text{ MPa}$ | | $\Delta\sigma_{N_i}/2 = 163 \text{ MPa}$ | | $\Delta\sigma_{N_i}/2 = 119 \text{ MPa}$ | |
| LM | PM | LM | PM | LM | PM | LM | PM |
| 122.5 MPa | 130.0 MPa | 64.0 MPa | 61.6 MPa | 143.7 MPa | 144.1 MPa | 126.6 MPa | 126.6 MPa |
| 40.0% | 48.6% | -20.5% | -23.4% | -11.8% | -11.6% | 6.4% | 6.4% |

The fatigue strength of any V-notched specimen can also be obtained with the proposed modelling, briefly described above and summarized in Fig. 1, after implementing the “direct” problem. Instead of the inverse search, the critical distance is known and the notch fatigue factor K_f is found, and then the stress amplitude deduced from the plain specimen fatigue limit. The details of this calculation, not reported here for brevity, can be retrieved in Santus et al. (2017). The sharp and the blunt specimen fatigue limit predictions are listed in Table 4. Again, in agreement with the accuracy map of Fig. 3 (b), when the critical distance is evaluated with the sharp specimen, the assessment of the blunt notch is quite accurate with errors on the order of 10%. On the contrary, the errors are significantly larger (20-40%) by assessing the sharp specimen strength with the critical distances deduced with the blunt specimen.

Apparently, LM and PM produced quite different results in terms of critical distances and, as mentioned above, the PM values are larger than the LM, Table 2. However, the LM critical distance was then used to assess the fatigue strength according to the LM for sharp and blunt specimens, and similarly for the PM, while for the crack threshold assessment this distinction vanishes. As evident in the lower part of Table 4, despite the different length values, the assessments obtained via LM and PM turn out to be very similar both for the blunt prediction from the sharp critical distance and vice versa.

Along the diagonal of the accuracy map of Fig. 3 (b), no experimental data is available and then an intermediate accuracy can only be conjectured. Obviously, if the same specimen were used to derive the critical distance and verify the assessment, a fictitiously perfect agreement would result. A significant test would be the assessment of a different geometry specimen, or a component, however with the same notch radius sharpness. On the other hand, if a different crack is assessed, there will be no need to convert the threshold into the critical distance through the plain specimen fatigue limit, since the threshold is already the fatigue strength for any long crack.

In conclusion, the most effective way to have good accuracy is to use a sharper notch for the critical distance length evaluation and then assess the fatigue strength of blunter notched components, with no significant effect in terms of LM or PM. If the design component notch is sharp itself, the threshold derived critical distance can be used, or again the sharp notch, which in the end can be considered effective for all cases.

6. Conclusions

- The critical distances of 42CrMo4+QT steel were experimentally determined with rounded V-notched specimens to test the recently proposed line and point method inverse search procedure.
- Crack threshold, plain and notched specimen experimental data was reported for load ratios -1 and 0.1, then allowing a series of comparisons both in terms of length values and fatigue strength assessments.
- The obtained critical distances were not very sensitive to small notch radius variations while dependent on the method, indeed the PM length was significantly larger than the LM one, however still producing quite similar predictions when assessing the fatigue strength.
- Since the critical distance was quite small for this investigated high strength steel, accurate fatigue assessments were only obtained with the sharp notch and the crack threshold derived critical distances. Therefore, the use of a blunt notch to find the material length and then the strength of higher sharpness notches, or even the crack threshold, is not recommended.

Acknowledgements

This work was supported by the University of Pisa under the “PRA – Progetti di Ricerca di Ateneo” (Institutional Research Grants) – Project No. PRA_2016_36.

References

- Araújo J.A., Susmel L., Taylor D., Ferro J.C.T., Mamiya E.N., 2007. On the use of the Theory of Critical Distances and the Modified Wöhler Curve Method to estimate fretting fatigue strength of cylindrical contacts, *International Journal of Fatigue* 29, 95–107.
- Benedetti M., Fontanari V., Allahkarami M., Hanan J., Bandini M., 2016. On the combination of the critical distance theory with a multiaxial fatigue criterion for predicting the fatigue strength of notched and plain shot-peened parts, *International Journal of Fatigue* 93, 133–147.
- Benedetti M., Fontanari V., Santus C., Bandini M., 2010. Notch fatigue behaviour of shot peened high-strength aluminium alloys: Experiments and predictions using a critical distance method, *International Journal of Fatigue* 32, 1600–1611.
- Bertini L., Santus C., 2015. Fretting fatigue tests on shrink-fit specimens and investigations into the strength enhancement induced by deep rolling, *International Journal of Fatigue* 81, 179–190.
- Santus C., Taylor D., Benedetti M., 2018. Determination of the fatigue critical distance according to the Line and the Point Methods with rounded V-notched specimen, *International Journal of Fatigue* 106, 208–218.
- Susmel L., Taylor D., 2010. The Theory of Critical Distances as an alternative experimental strategy for the determination of K_{Ic} and ΔK_{th} , *Engineering Fracture Mechanics* 77, 1492–1501.
- Taylor D., 2007. *The Theory of Critical Distances: A New Perspective in Fracture Mechanics*, Elsevier, Oxford, UK.
- Taylor D., 2008. The theory of critical distances, *Engineering Fracture Mechanics* 75, 1696–1705.
- Taylor D., 2011. Applications of the theory of critical distances in failure analysis, *Engineering Failure Analysis* 18, 543–549.